ELSEVIER

Journal of Nuclear Materials 313–316 (2003) 604–608

journal of nuclear materials

www.elsevier.com/locate/jnucmat

Computer modeling of ion implanted deuterium release from tungsten

A.A. Pisarev *, I.D. Voskresensky, S.I. Porfirev

Department of Physics, Moscow Engineering and Physics Institute, Kashirskoe shosse 31, Moscow 115409, Russia

Abstract

Computer modeling of hydrogen release from tungsten during and after ion implantation was made. The model was based on diffusion equation with hydrogen-defect interaction and desorption from the chemisorption state taken into account. One particular experiment on re-emission during implantation, desorption decay after implantation followed by programmed thermodesorption was thoroughly analyzed. Influence of the model parameters, such as diffusivity, solubility, the rate of defect production, maximum concentration of defects, binding energy, and activation energy for chemisorption was analyzed. The set of the best fit parameters was found that gave a good overall description of all three stages of the experiment.

PACS: 52.40.Hf
Keywords: Hydrogen; Tungsten; Ion trapping; Diffusion; Defects; Desorption

1. Introduction

Investigation of hydrogen trapping and release is important for analyses of tritium aspects in the thermonuclear reactor. Numerical calculations based on computer codes like PERI [1], DIFFUSE [2], and TMAP [3] are often used both for description of laboratory experiments and predictions of fuel behavior in the reactor. Unfortunately, computer modeling often gives only general tendencies of release. This situation is typical for tungsten recently proposed as a material for the baffle and divertor. For example, modeling of re-emission in [4,5] gives too fast rise, modeling of TDS in [6,7] gives a wrong shape of the peaks: they are broader in [6] and narrower in [7] than in the experiment. This work is devoted to analysis of ability of modeling to describe thoroughly an experiment. For this purpose, we take just one experiment on ion implantation, which consists of three stages: re-emission during ion implantation, release after termination of implantation, and programmed desorption. We will demonstrate good agreement of the experiment and calculations for the three stages and then analyze influence of some model parameters.

2. Mathematical model

The model is based on the commonly used diffusion equation with a source determined by ion implantation and a sink determined by hydrogen-defect interaction.

$$\frac{\partial u(x,t)}{\partial t} = D\frac{\partial^2 u(x,t)}{\partial x^2} + I_0\varphi(x) - S_{\sum}(x,t),$$

Hereafter, 'hydrogen' means any hydrogen isotope, $I_0(\mathrm{H}^+/\mathrm{cm}^2\,\mathrm{s})$ – the ion flux penetrating the metal, $u(x,t)$ – the bulk concentration of mobile hydrogen in interstitials, D – the diffusion coefficient, $\varphi(x,t)$ – the ion stopping profile, $S_{\sum}(x,t)$ – the defect trapping sink. Defects could be of different types depending on experimental conditions, therefore several types of defects, which are traps for hydrogen, can co-exist with their

* Corresponding author. Tel.: +7-095 323 9325; fax: +7-095 324 7024.
E-mail address: pisarev@plasma.mephi.ru (A.A. Pisarev).

0022-3115/03/$ - see front matter
PII: S0022-3115(02)01434-4

partial trapping–detrapping terms S_k, which can be written in the classical way:

$$S_{\sum}(x,t) = \sum_k S_k(x,t),$$

$$S_k(x,t) = 4\pi R_k D\left[u(w_k - y_k) - y_k N \xi e^{-E_{bk}/kT}\right],$$

here R_k – the radius of trapping in the defect, ξ – the number of sites available for the hydrogen atom in solution around the trap, N – the atomic density of the metal, $w_k = w_k(x,t)$ – the total concentration (filled plus empty) of traps, and E_{bk} – the binding energy. Index k refers to the kth type of defects.

The hydrogen concentration in defects of the kth type changes as

$$\partial y_k(x,t)/\partial t = S_k(x,t).$$

The concentration of defects is a function of the depth and time. It is reasonable to suggest that $w_k(x,t)$ increases with the ion fluence until some maximum level w_{km} (cm^{-3}) is achieved.

$$w_k(x,t) = w_{km}\{1 - \exp[-I_0 t\gamma_k \psi_k(x,t)/w_{km}]\},$$

here γ_k (defects/ion) is the number of defects created by every incident ion, ψ_k – the profile of defects created. One must mention that $w_k(x,t)$ is the concentration of defects if only one atom can be trapped in every defect. Otherwise, $w_k(x,t)$ is a product of the real concentration of defects and the number of atoms that can be trapped in one defect of the kth type.

Desorption of hydrogen from a metal is usually considered as a product of the squared under-the-surface concentration and an effective recombination coefficient: $J_{des} = K_r u(0,t^2)$. In our model, along with atoms in the bulk, we introduce chemisorption states on the surface and consider desorption from these states as $J_2 = n^2 \nu \lambda^2 \exp[-2(E_c - Q_c)/(kT)]$ ($\mathrm{H_2/cm^2\,s}$), where n (cm^{-2}) is the concentration of particles in these states, ν is the vibration frequency of atoms, λ – the lattice parameter, E_c – activation energy for chemisorption, Q_c – heat of chemisorption. Particles can exchange between the chemisorption sites and bulk sites with the rates $J_3 = n\nu \exp[-(E_s - Q_c)/(kT)]$ and $J_4 = (1 - n/n_m)u\nu\lambda \times \exp[-(E_s - Q_s)/(kT)]$, where E_s is surface barrier for absorption. Q_s – heat of solubility, and n_m – the concentration of chemisorption states.

The boundary conditions for n and u for solving the diffusion equation can be obtained from the balance of particles:

$$\lambda\partial u(x,t)/\partial t = J_3 - J_4 - J_d - S_{\sum}(0,t)\lambda + I_0\varphi(0)\lambda, \quad x = 0,$$

$$\partial n(t)/\partial t = -2J_2 + J_4 - J_3 - S_{\sum}(0-\lambda,t)\lambda + I_0\varphi(0-\lambda)\lambda, \quad x = 0-\lambda,$$

$$\lambda\partial u(x,t)/\partial t = J_3 - J_4 + J_d - S_{\sum}(L,t)\lambda + I_0\varphi(L)\lambda, \quad x = L,$$

$$\partial n(t)/\partial t = -2J_2 + J_4 - J_3 - S_{\sum}(L+\lambda,t)\lambda + I_0\varphi(L+\lambda)\lambda, \quad x = L+\lambda,$$

here $J_d = -D\partial u/\partial x$ – the diffusion flux. The system of equations was solved numerically.

3. Results and discussion

Experiments, which were taken for modeling, were performed with 15 keV D_2^+ ions at the ion flux $I_0 = 8.75 \times 10^{13}$ $\mathrm{D_2/cm^2\,s}$ and the temperature of 473 K during implantation. The rate of programmed heating after implantation was 4.8 K/s. Three stages of the experiment are shown in Fig. 1. One can see that the calculations reproduce all the three stages of the experiment rather well. The diffusivity and solubility were taken from Frauenfelder [8] $D(T) = 4.1 \times 10^3 \exp(-0.39\ \mathrm{eV}/kT)$ $\mathrm{cm^2\,s^{-1}}$, $S(T) = 1.78 \times 10^{18} \exp(-1.04\ \mathrm{eV}/kT)$ at $\mathrm{cm^{-3}\,Pa^{-1/2}}$. Parameters describing defects and surface were varied. A good overall fit of three stages of the experiment was obtained in calculations with two types of defects with $E_B = 0.7$ and 1.05 eV, $\gamma = 1.0$ defects/ion for both, and $w_m = 10^{20}$ and 3×10^{20} defects/$\mathrm{cm^3}$. The chemisorption parameters were adjusted at $Q_c = -0.3$ eV, $E_c = 0.34$ eV. The barrier for absorption $E_s = 1.43$ eV was taken as a sum of the heat of chemisorption and the activation energy for diffusion. The parameters, which are given in literature for w, are very uncertain and depend on experimental conditions as it was analysed for example in the recent overview made by Causey [9]. Therefore in this short paper, we will not discuss physics connected with the values obtained, for example,

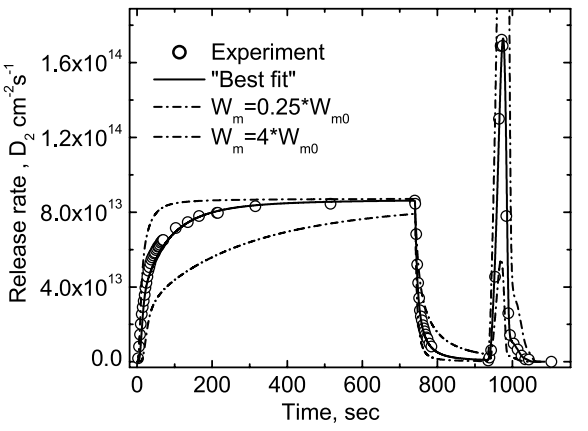

Fig. 1. Experiment (dots) and calculations (lines) of ion implanted deuterium release. Solid line – the best fit. Dashed lines are obtained with other values of the maximum concentration of all types of defects.

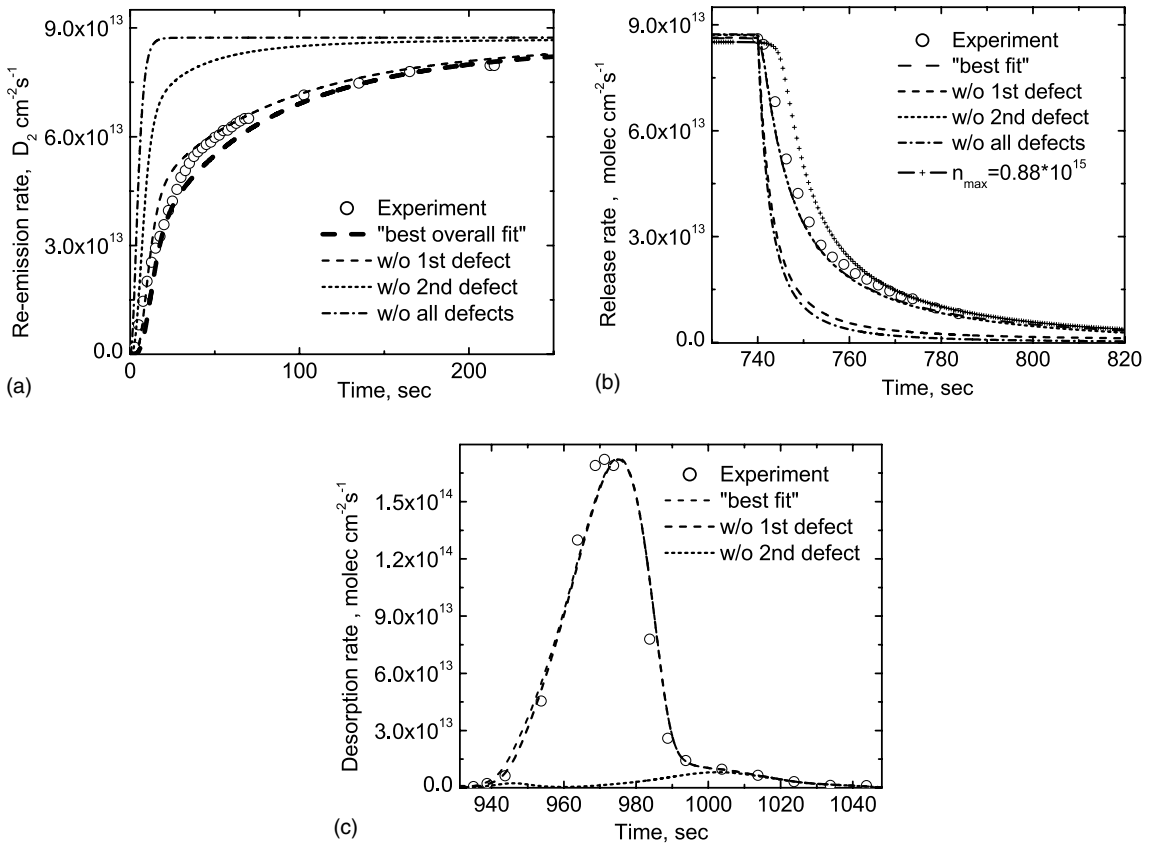

Fig. 2. Re-emission during ion implantation (a), release after termination of implantation (b), and programmed thermodesorpion (c). Dots – experiment, lines – calculations. Solid line – the 'best fit' with five types of defects. Other lines – without one or all defects.

the types of defects and conditions of their production, influence of impurities on the surface barriers and heats, etc. One must only state that the values obtained do not contradict anything.

Thermodesorption spectrum (TDS) in Figs. 1 and 2(c) consist of only one distinct peak, which corresponds to 1.05 eV defects. Besides, re-emission is described well without 0.7 eV defects in Fig. 2(a). Therefore, one could decide that only 1.05 eV defects are enough for a good description. But this was found to be wrong as Fig. 2(b) shows: if calculations were performed without 0.7 eV defects, the decay of release after implantation went too fast. Existence of defects with a lower energy was proved in supplementary experiments performed at 373 K, where two additional low temperature peaks appeared, which were well modeled by release from solid solution and defects with $E_B = 0.7$ eV. At 473 K implantation, concentration in the solid solution and these defects is very small; therefore the respective peaks do not appear in TDS.

The only detail, which has not been reproduced with two types of defects, is a small step on the high temperature wing of the TDS. This step can be modeled by introduction of several additional defects with $E_B = 1.5$–2 eV. The total maximum concentration in these defects is about 10^{19} cm^{-3}, and the total rate of their production is about 1.5 defects/ion

Fig. 2(a) contains also plots without the second defects and without defects at all. One can see that re-emission rises too fast in this case. This observations as well as analyses of concentrations in solid solution and defects show that defect trapping is the main mechanism of ion implanted deuterium accumulation.

Fig. 2(b) demonstrate the situation opposite to that in Fig. 2(c): if to abolish 1.05 eV defects the decay does not change, while 0.7 eV defects are important. The explanation is rather simple: defects with the higher binding energy are totally populated and the detrapping probability is negligible at the temperature of implantation. Therefore, they neither trap nor detrap deuterium at 473 K after termination of implantation. This is why they have no influence on the decay curve. As for 0.7 eV defects, they actively participate both in trapping and detrapping at this temperature. And the resulting effect is decrease of hydrogen transport to the surface. If to set the concentration of these defects to zero, their

trapping effect vanishes, the hydrogen transport rate increases, and decay of re-emission goes faster.

The binding energies strongly influence the positions of the TDS peaks and are choosen mainly by fitting TDS. The shapes of the re-emission and the decay stages also depend of E_B values. These two stages are also influenced by the maximum concentration of defects and the rate of their production. Fig. 1 demonstrates what happens if the concentrations of all defects is either increased or decreased four times. Increase of w_m retards desorption during and after ion implantation and mounts the height of the TDS peaks.

Influence of the rate of defect production γ is shown in Fig. 3. This figure is plotted for the model case of a single type of defects. It is obvious that the rate of defect production is important factor only at low fluences where defect concentration depends on γ. Increase of γ must retard re-emission in the initial stage of implantation. At high fluences where w approaches to w_m, γ values are not so important. Therefore increase of γ retards the start of re-emission; and at $\gamma = 3$ it looks like a breakthrough after some lag time.

Two peculiar effects are additionally observed in Fig. 3. The first one is a step at the most low fluences, which appears at $\gamma \geqslant 2$. The step like that was observed in many experiments with various materials, and it was explained as a consequence of ion reflection. Our calculations demonstrate that there is another reason not connected with reflection: at the very beginning of implantation, when the concentration of defects is still very low, some of implanted atoms can avoid trapping into defects and diffuse towards the surface where they rapidly desorb. The higher the defect production rate, the lower the height and the longer the length of the step. At low γ, the jump is faster and higher, but the step is not pronounced. Instead, at low γ, the second feature is seen:

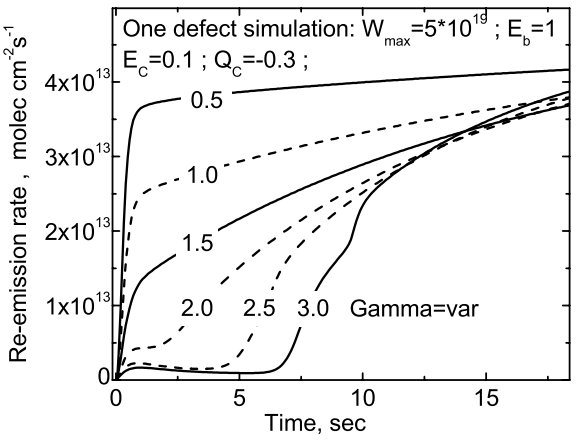

Fig. 3. Re-emission rate during ion implantation calculated for various rates of defect production. Only one type of defects was taken for modeling. The values of E_B, E_c, and Q_c are given in eV.

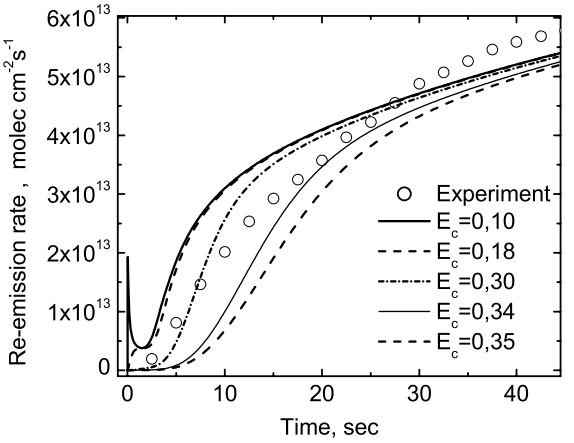

Fig. 4. Re-emission rate measured experimentally (dots) and calculated at various energies for chemisorption. The values of E_c are given in eV.

re-emission slowly rises after the rapid jump. This effect, which we have also observed in some experiments, can be misunderstood as a rise of the background. But this is not true: re-emission is still at the level of 0.5 in this figure.

Surface properties are also important in gas release. Fig. 4 shows influence of the activation energy for chemisorption. The higher E_c the stronger suppression of re-emission. Influence of surface parameters is not so strong as that of defects; nevertheless, E_c adjusting is necessary as the influence of surface and defects on the shape of the curves is different. Fig. 4 also demonstrates the step in the very beginning of implantation at $E_c \approx 0.18$ eV. That is, this feature depends also on surface conditions. At a very low E_c a peak of re-emission appear, which has never been observed experimentally and therefore gives a lower margin of E_c values, which are worth to be considered.

An interesting effect has been observed just after termination of implantation: there is a lag time of re-emission decay of the order of a few seconds. This effect was shown to depend on surface effects. It appears when surface population during implantation becomes very high. In the case $n/n_m \to 1$, the concentration under the surface drastically increases to ensure high J_4 at low $(1 - n/n_m)$. After termination of implantation in this case, the number of under-surface atoms feeding the on-surface sites remains high for as longer time, and this gives delay in $n(t)$ decrease. A decay curve at a low n_m is shown for comparison in Fig. 2(b).

4. Conclusion

Modeling of deuterium release during and after ion implantation has given a very good agreement with

experiment. Three stages of release (re-emission during implantation, release decay after termination of implantation, and programmed thermodesorption) have been well described. The diffusivity and solubility were taken fixed and only influence of parameters characterizing defects and surface was investigated.

A good overall fit was obtained in calculations with two types of defects with the binding energies $E_B = 0.7$ and 1.05 eV, the rates of defect production $\gamma = 1.0$ defects/ion both, and the maximum concentrations $w_m = 10^{20}$ and 3×10^{20} defects/cm^3. A small amount (10^{19} cm^{-3}) of defects with higher binding energies of 1.5–2.0 eV must be also suggested to describe a small high temperature feature of thermodesorption spectrum. The chemisorption heat and activation energy were adjusted at $Q_c = -0.3$ eV and $E_c = 0.34$ eV.

The defect trapping has been shown to be the main mechanism of deuterium accumulation.

Some features of release have been demonstrated. Particularly, at high rate of defect production, a delay of re-emission is observed followed by a sudden breakthrough of release. At the defect production rate >2, a step in the very initial part of the re-emission curve has been found, which looks like the reflection of ions but is connected with low concentration of defects at low fluence. At low γ, the re-emission rate rapidly jumps to a high level and then slowly increases, which can mislead in the experiment being accepted as the backgroind rise.

Surface properties are also important. The higher the activation energy for chemisorption E_c the stronger suppression of re-emission. At intermediate $E_c \approx 0.18$ eV, a step of re-emission, which also looks as a reflection feature has also been observed. At a very low E_c a peak of re-emission appears, which has never been observed experimentally and therefore gives a lower margin of E_c worth to be considered.

The experiment and modeling give a delay of desorption decay after termination of irradiation, which is connected with high population of the chemisorption sites at the end of the implantation stage.

Acknowledgement

This work was made thanks to the Contract 12138/R0/RBF with International Atomic Energy Agency.

References

[1] P. Wienhold et al., IPP Kernforschungsanlage, Jülich, Report 1825 (1983).
[2] M.I. Baskes, Sandia National Laboratories, Preprint SAND 83-8231, 1983.
[3] G.R. Longhurst, D.F. Holland, J.L. Jones, B.J. Merill, TMAP4 Users Manual, Idaho National Engineering Laboratory, EGG-FSP-10315, 1992.
[4] P. Franzen, C. Garcia-Rosales, H. Plank, V.Kh. Alimov, J. Nucl. Mater. 241–243 (1997) 1082.
[5] R.A. Anderl, D.F. Holland, G.R. Longhurst, et al., Fus. Technol. 21 (1992) 745.
[6] F.C. Sze, R.P. Doerner, S. Luckhard, J. Nucl. Mater. 264 (1999) 89.
[7] T.J. Venhaus, R.A. Causey, Fus. Technol. 39 (2001) 868.
[8] R. Frauenfelder, J. Vac. Sci. Technol. 6 (1969) 388.
[9] R. Causey, J. Nucl. Mater. 300 (2002) 91.